Evidence for Charge Orbital and Spin Stripe Order in an Overdoped Manganite

H. Ulbrich,[1] D. Senff,[1] P. Steffens,[2] O. J. Schumann,[1] Y. Sidis,[3] P. Reutler,[4] A. Revcolevschi,[4] and M. Braden[1]

[1]*II. Physikalisches Institut, Universität zu Köln, Zülpicher Strasse 77, D-50937 Köln, Germany*
[2]*Institut Laue-Langevin (ILL), B.P. 156, 38042 Grenoble Cedex 9, France*
[3]*Laboratoire Léon Brillouin (LLB), C.E.A./C.N.R.S., F-91191 Gif-sur-Yvette Cedex, France*
[4]*Laboratoire de Chimie des Solides, LPCES - ICMMO, Université de Paris Sud XI, 91405 Orsay, France*

(Received 20 August 2010; published 12 April 2011)

Overdoped $La_{0.42}Sr_{1.58}MnO_4$ exhibits a complex ordering of charges, orbitals, and spins. Neutron diffraction experiments reveal three incommensurate and one commensurate order parameters to be tightly coupled. The position and the shape of the distinct superstructure scattering as well as higher-order signals are inconsistent with a harmonic charge and spin-density-wave picture but point to a stripe arrangement in which ferromagnetic zigzag chains are disrupted by excess Mn^{4+}.

DOI: 10.1103/PhysRevLett.106.157201 PACS numbers: 75.25.Dk, 71.10.−w, 75.47.Lx, 75.50.Ee

In the stripe phases [1] additional charges segregate into stripes so that an antiferromagnetic (AFM) order in between is conserved. The stripe scenario, which can be considered as a soliton lattice, is of general relevance in the physics of doped Mott insulators with similar stripe patterns being reported in cuprates, nickelates, and cobaltates [1–4]. Evidence of incommensurate ordering of charges and orbitals has also been observed for various manganites at high doping levels, i.e., overdoped with respect to half doping with stable charge and orbital ordering (COO), but a clear picture, in particular, the coupling to the magnetism, is still missing in spite of strong efforts [5–20].

Electron diffraction experiments reported the incommensurate modulations to linearly follow the amount of extra charges [5–7] yielding the first evidence for stripe phases. Meanwhile, numerous electron, x-ray, and neutron diffraction experiments studied overdoped manganites, however, without reaching a clear conclusion [8–12,18,20]. The intrinsic nature of the structural phases remains a matter of controversy, as both a soliton lattice reflecting the stripe pattern [13,14] and a homogenous charge-density wave [10,16] have been proposed.

This work aims to elaborate a consistent model for charge, orbital, and magnetic order in overdoped manganites. Three incommensurate order parameters associated with charges, orbitals, and Mn^{3+} spins, respectively, and one commensurate order parameter are tightly coupled with each other, yielding a stripe-type arrangement of charges and zigzag fragments of magnetic order.

Neutron diffraction experiments were performed on the instruments 3T.1 and G4.3 at the LLB ($E = 14.7$ meV) and on the triple-axis spectrometer IN20 at the ILL. On IN20, the flat-cone detector with silicon (111) analyzers fixes the final energy to 18.7 meV. In all experiments, the c axis was set vertical to the diffraction plane. Magnetization was measured by a SQUID magnetometer and electric resistivity by a standard four-contact technique (Fig. 1).

Large single crystals of $La_{1-x}Sr_{1+x}MnO_4$ with $x = 0.5$ and $x = 0.58$ were grown by the floating-zone technique [21]. The $x = 0.5$ sample was already used in previous experiments [22,23]. X-ray single-crystal diffraction indicates a slightly lower Sr content than the nominal composition of the starting rod in the crystal growth: $x = 0.6$ [21]. The transition into the COO state ($T_{CO} = 255$ K for $x = 0.58$) manifests itself by the appearance of superstructure reflections as well as by a sharp drop of the magnetization; see Fig. 1. The AFM ordering, however, is not visible in the macroscopic data due to a strong 2D character. Magnetic superstructure reflections are detected below $T_N \approx 95$ K in agreement with Ref. [19], but the transition is sluggish.

The ordered phases in $La_{0.5}Sr_{1.5}MnO_4$ have been characterized by using various methods [18,23,24] focusing on the structural distortion. With the flat-cone detector we may easily map the $(h, k, 0)$ plane and identify the different signals. Four order parameters can be separated; see Ref. [23]. Proper charge ordering of the checkerboard type is related to a mode at $\mathbf{k}_{co} = \pm(0.5, 0.5)$ (referring to the two-dimensional space and thus neglecting

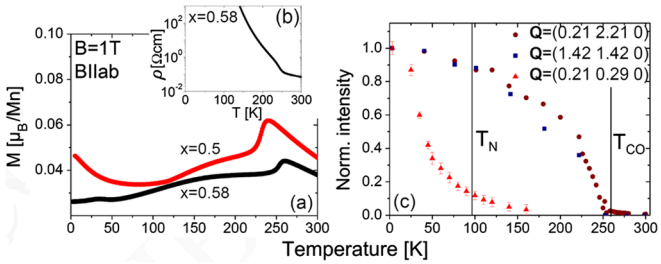

FIG. 1 (color online). Temperature dependence of magnetization for a field of 1 T applied parallel to the ab planes for $x = 0.5$ and 0.58 (a). The inset presents the in-plane electric resistivity for $x = 0.58$ (b). For $La_{0.42}Sr_{1.58}MnO_4$, characteristic superstructure reflections increase in intensity at the transition temperatures into the COO state and into the AFM state, respectively (c).

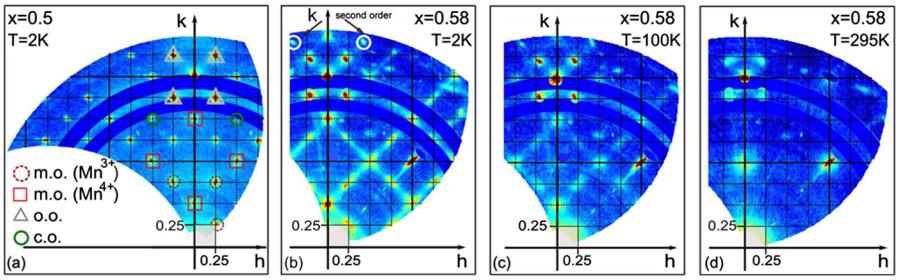

FIG. 2 (color online). Distribution of structural and magnetic scattering in the $(h, k, 0)$ plane for $La_{0.5}Sr_{1.5}MnO_4$ and $La_{0.42}Sr_{1.58}MnO_4$. For $x = 0.5$ superstructure reflections refer to the charge (green circles), orbital (gray triangles), and magnetic ordering (Mn^{3+}: dotted circles; Mn^{4+} red squares) (a). The ordered state for $x = 0.58$ is governed by an incommensurate ordering of charge, orbital, and magnetic ordering of Mn^{3+} (b). Slightly above the Néel temperature T_N, the magnetic superstructure reflections vanish but a diffuse magnetic signal is still visible (c). At room temperature, diffuse signals exist around the Bragg reflections $\mathbf{Q} = (0, 2, 0)$ and $\mathbf{Q} = (0, 1, 0)$ (d). Contaminations from a crystallite and from the Al sample holder are covered in blue color.

interlayer coupling). The orbital ordering causes an additional doubling along one direction and is associated with a mode at $\mathbf{k}_{oo} = \pm(0.25, 0.25)$. The magnetism is described by two propagation vectors $\mathbf{k}_{Mn^{3+}} = \pm(0.25, -0.25)$ and $\mathbf{k}_{Mn^{4+}} = \pm(0.5, 0.0)$ referring to the nominal Mn^{3+} and Mn^{4+} spins, respectively. In the scattering map in Fig. 2(a), one may thus easily attribute each superstructure scattering with the associated order parameter. Also, for the quarter-indexed peaks the identification is unambiguous due to the distinct $\mathbf{Q}$ dependence of magnetic and structural scattering.

Figure 2(b) illustrates the same area of reciprocal space at $T = 2$ K for the overdoped system $La_{0.42}Sr_{1.58}MnO_4$, and Fig. 3 shows single-counter scans. The inspection of the two scattering maps immediately shows similar ordering phenomena, but, instead of the sharp signals at commensurate $\mathbf{Q}$ positions, there are broader features mostly centered at incommensurate positions in $La_{0.42}Sr_{1.58}MnO_4$. The direct comparison allows one to identify three underlying ordering schemes. Superstructure reflections referring to the charge ordering are centered, for example, at $\mathbf{Q} = (1.5 + \delta_{co}, 1.5 + \delta_{co})$ with $\delta_{co} = 0.080(3)$. The incommensurability δ_{co} does not change with temperature as scans parallel to the modulation exhibit only the thermal suppression of intensity; see Fig. 3(a). Superstructure reflections associated with the orbital ordering are incommensurate as well, in agreement with previous x-ray experiments [18]. The orbital satellites are centered closer to the Bragg reflection, for example, $\mathbf{Q} = (0, 2, 0)$ in the diagonal direction. At this $\mathbf{Q}$ range, magnetic scattering can be fully neglected due to the magnetic form factor. The orbital scattering is incommensurately displaced towards the central Bragg peak, $\mathbf{k}_{oo} = (0.25 - \delta_{oo}, 0.25 - \delta_{oo})$, and again there is no temperature dependence [Fig. 3(b)]. The incommensurability of the orbital satellites is within the error bars exactly half of that of the charge ordering [$\delta_{oo} = 0.039(2) = \frac{1}{2}\delta_{co}$]. These observations reveal the tight coupling between charge and orbital ordering in $La_{0.42}Sr_{1.58}MnO_4$, and they perfectly agree with previous diffraction studies [5–12,18]. Most interestingly, we clearly observe second-order harmonics of the orbital signal.

The quarter-indexed scattering associated with Mn^{3+}-spin ordering is split in $La_{0.42}Sr_{1.58}MnO_4$. The incommensurate modulation of the Mn^{3+}-spin order is transverse with respect to the Mn^{3+} order in $x = 0.5$ (but note it is parallel to the chains) $\mathbf{k}_{Mn^{3+}} = (0.25 - \delta_{Mn^{3+}}, 0.25 + \delta_{Mn^{3+}})$ [see Figs. 2(b) and 3(c)], and it does not exhibit a significant temperature dependence. Longitudinal scans yield a peak centered at the commensurate position due to the overlap of the two incommensurate contributions.

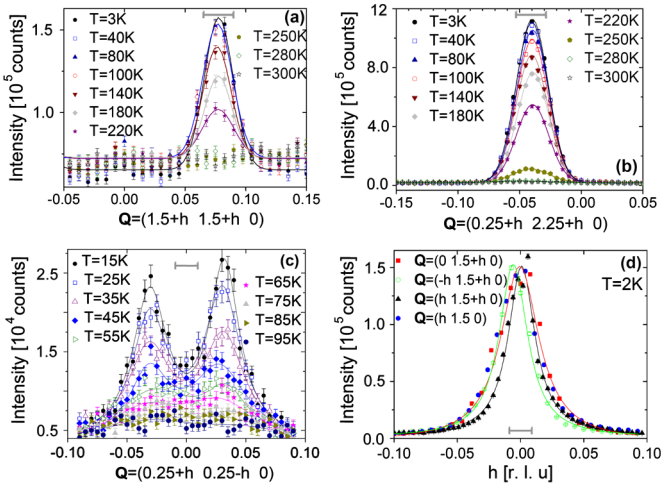

FIG. 3 (color online). Single-counter scans across the different superstructure peaks; intensities were scaled to the low-temperature peak heights in the flat-cone data. Satellites referring to the charge ordering (a) are displaced twice as much as those of orbital ordering (b) and of Mn^{3+} spin ordering (c), respectively. Reflections related to the magnetic ordering of Mn^{4+} appear at commensurate positions (d). The lines in (a) and (b) correspond to fits with Gaussian, while the lines referring to magnetic ordering in (c) and (d) correspond to fits with Lorentzians. The data in (c) are taken on G4.3, while data in (a), (b), and (d) are taken on 3.T1 (horizontal bars give the respective resolution).

The incommensurate character of the magnetic order was overlooked in Ref. [19] due to a wrong scan direction. With this incorrect assignment of magnetic order, it has been impossible to develop a model reconciling magnetic, orbital, and charge superstructures so far. From several magnetic superstructure reflections we determine the incommensurability $\delta_{Mn^{3+}}$, which perfectly agrees with the incommensurability of the orbital ordering: $\delta_{Mn^{3+}} = 0.037(2) = \delta_{oo} = \frac{1}{2}\delta_{co}$. These three independent order parameters are all incommensurate and tightly coupled to each other.

The magnetic scattering associated with the ordering of Mn^{4+} spins is centered at the same positions as those in $La_{0.5}Sr_{1.5}MnO_4$ (see Fig. 2), but the scattering in $La_{0.42}Sr_{1.58}MnO_4$ exhibits diffuse tails along the [110] direction. Additional scans were performed across the commensurate position $\mathbf{Q}_{Mn^{4+}} = \pm(0.0, 1.5)$ in horizontal, vertical, and diagonal directions. None of them indicates a sizable incommensurability. Therefore we may safely exclude that the Mn^{4+}-spin scattering exhibits an incommensurate shift comparable to those of the other three order parameters.

Having established the main characteristics of the four ordering schemes, we may develop a consistent model of the charge, orbital, and magnetic order in the overdoped manganite. Because of the intensity mapping of (hkl) planes with $l = 0$, 0.25, 0.5, and 1, it is ascertained that all superstructure signals have been detected. Since all scattering can be associated with the commensurate signals for $x = 0.5$, the order in $La_{0.42}Sr_{1.58}MnO_4$ must correspond to a modulation of the well established order at half doping. Charge and orbital superstructures peak at $l = 0$ and 1, whereas the magnetic order is of two-dimensional character, which is not astonishing in view of the fact that the stacking of magnetic planes remains ill-defined even for the most stable order at half doping [23,24]. Since all three observed incommensurabilities appear along the diagonal, the extra Mn^{4+} arrange in stripes along the diagonals as already deduced from the orbital reflections. This arrangement resembles the stripe phases in cuprates, nickelates, and cobaltates [1–4] and corresponds to a soliton lattice. We may further deduce from the orbital incommensurate modulation, which is longitudinal in nature, that the disruption of the orbital order occurs along the zigzag chains or, in other words, that the Mn^{4+} stripes align perpendicular to the chains. The magnetic superstructure reflections are in perfect agreement with this model if the magnetic order forms ferromagnetic zigzag fragments as shown in the real-space model in Fig. 4(a). The magnetic propagation vector $\mathbf{k}_{Mn^{3+}}$ points exactly perpendicular to the zigzag chains at half doping, so that the arrangement of the Mn^{4+} stripes perpendicular to the zigzag chains results in a transverse modulation of the corresponding magnetic order.

The commensurate scattering associated with the Mn^{4+} spins at $\mathbf{k}_{Mn^{4+}}$ can be easily explained. The magnetic

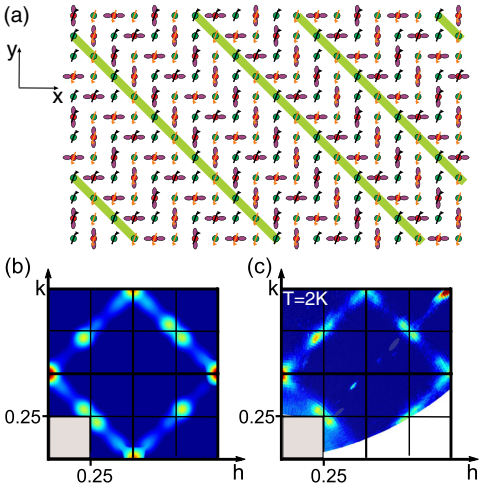

FIG. 4 (color online). Sketch of charge, orbital, and spin order for $La_{0.42}Sr_{1.58}MnO_4$ (a). Red circles represent Mn^{3+} and green circles Mn^{4+}. A single domain of zigzag chains propagating in the [110] direction is shown. The excess lines of Mn^{4+} are displayed on a green background. The Fourier transformations superposed for all domains (b) agree with the experimental map obtained at $T = 2$ K (c) [25]. Note that the intensity at the position $Q = (1, 1, 0)$ in (c) is a Bragg peak.

structure in the zigzag fragments follows the strong ferromagnetic interaction across the Mn^{3+} orbitals. However, this does not fix the coupling in the double line of Mn^{4+}. Ferromagnetic Mn^{4+}-spin pairs in these double lines may align either horizontally or vertically [the vertical solution is shown in Fig. 4(a)], but all these pairs must align in the same sense in order to explain the commensurate Mn^{4+} signal. Taking into account the possible orientations of the Mn^{4+} stripes along the two diagonals of the tetragonal lattice, we obtain four monoclinic magnetic domain orientations whose scattering contributions superpose. This magnetic structure perfectly explains the commensurate $\mathbf{k}_{Mn^{4+}}$ intensities, as the Mn^{4+} spins sum up along the vertical bond direction and alternate in the horizontal direction resulting in magnetic scattering at $\mathbf{Q} = (0.5, 0)$ for the domain chosen in Fig. 4(a).

In order to analyze the position and the shape of the different scattering contributions, we performed two-dimensional Fourier transforms of large supercells (typically 380×380 lattices) in which the charge, orbital, and spin order were implemented schematically. If we calculate the average incommensurability of orbital, of magnetic (Mn^{3+}), and half that of charge ordering, we obtain $\bar{\delta} = 0.039(2)$, which via the scaling relation $\epsilon(x)$ indicates a Sr content $x = 0.58$. This value perfectly agrees with the determination by x-ray diffraction. The concentration $x = 0.58$ cannot be realized by an adjustment of stripes with equal distances but by a mixture of 33% blocks being arranged according to $x = 0.6$ and 66% blocks with $x = 0.57$. The entire modulation consists thus of an alternation of blocks with seven lattice-spacings length and with five lattice-spacings length with a ratio of 2:1 [see

Fig. 4(a)]. The structural arrangement corresponds to a soliton lattice in which only the average soliton distance is defined. The supercells of about 380×380 lattices are larger than the correlation lengths of the ordering in these manganites (and also larger than the neutron coherence length) so that finite-size effects can be neglected. The Fourier transform of the superposition of the four domains explains the appearance of all the scattering observed. By taking into account the direction of the spins, the intensity of the magnetic signals can be adjusted [25]. The experimental maps indicate that the magnetic scattering is not sharp but exhibits diffusive tails along the diagonal concerning both the Mn^{4+} and the Mn^{3+} contributions; this effect is perfectly reproduced by the Fourier transform as well. Magnetic order in the direction parallel to the stripes is perfect on a large length scale, but in the direction perpendicular to the stripes, magnetic order is regularly perturbed by the soliton generating diffuse tails. Such an anisotropic broadening was shown to yield direct evidence for a stripe arrangement [26]. The sharper main response for the Mn^{4+} spin scattering arises from the fact that Mn^{4+} spin order passes the domain wall. The perfect agreement between the simulated and the experimental scattering maps [see Figs. 4(b) and 4(c)] [25] including the diffuse tails gives strong evidence for the stripe arrangement and excludes a homogeneous spin- and charge-density-wave modulation. This conclusion is further corroborated by the observation of second-order harmonics of the orbital superstructure scattering. The squaring up of a density wave is usually associated with third-order harmonics, but for the orbital pattern there is no squaring up, but a strong pair or triple of opposite orbital phases (associated with a single ''zig'' in the chains) is surrounded by suppression of orbital order in the Mn^{4+} rows. This arrangement yields strong second-order harmonics. Evidence for a magnetic soliton arrangement in overdoped manganites was recently obtained by NMR experiments [17].

Above T_N, we still observe a diffuse magnetic signal around the quarter- and half-indexed positions [see Fig. 2(c)], which rapidly loses intensity upon further heating, while a ferromagnetic signal appears [see Fig. 2(c)]. In the scattering map taken above the COO state [see Figs. 2(d) and 3] the AFM scattering is fully lost. Instead of that, ferromagnetic correlations appear around $\mathbf{Q} = (0, 1, 0)$ reflecting the increase of the macroscopic magnetization; see Fig. 1(a). The competition between ferromagnetic short-range correlations and AFM order, reported for $La_{0.5}Sr_{1.5}MnO_4$ [22,23], persists in the overdoped concentration range.

The orbital and charge order scattering does not change when heating above the magnetic transition [see Fig. 2(c)]. Although the charge scattering apparently fully disappears at T_{CO}, diffuse orbital scattering is still visible at $T = 295$ K, i.e., well above the COO transition, where it remains clearly incommensurate. The charge and orbital disordered state thus already exhibits the instability against incommensurate orbital ordering with the position fixed through the amount of doping. The incommensurate orbital instability thus cannot be caused by the magnetic correlations, as it coexists with dominant ferromagnetic correlations.

In conclusion, the charge, orbital, and spin ordering in a layered overdoped manganite, $La_{0.42}Sr_{1.58}MnO_4$, was studied by neutron diffraction. With the flat-cone detector we obtain the full scattering of four order parameters that are tightly coupled. While the ordering of charges, orbitals, and Mn^{3+} spins is incommensurate, the Mn^{4+} spins order in a commensurate pattern. The full scattering maps including the positions and the diffuse shape of the superstructure intensities are well described by a stripe-type arrangement where the excess Mn^{4+} spins form stripes disrupting the ferromagnetic zigzag chains. This picture is corroborated by second-order harmonics observed for the orbital superstructure.

This work was supported by the Deutsche Forschungsgemeinschaft through the Sonderforschungsbereich 608.

[1] J. M. Tranquada *et al.*, Nature (London) **375**, 561 (1995).
[2] J. M. Tranquada, D. J. Buttrey, and V. Sachan, Phys. Rev. B **54**, 12 318 (1996).
[3] R. Kajimoto *et al.*, Phys. Rev. B **64**, 144432 (2001).
[4] M. Cwik *et al.*, Phys. Rev. Lett. **102**, 057201 (2009).
[5] A. P. Ramirez *et al.*, Phys. Rev. Lett. **76**, 3188 (1996).
[6] S. H. Chen *et al.*, J. Appl. Phys. **81**, 4326 (1997).
[7] S. Mori *et al.*, Nature (London) **392**, 473 (1998).
[8] R. Wang *et al.*, Phys. Rev. B **61**, 11 946 (2000).
[9] T. Kimura *et al.*, Phys. Rev. B **65**, 020407 (2001).
[10] J. C. Loudon *et al.*, Phys. Rev. Lett. **94**, 097202 (2005).
[11] Z. P. Luo, D. J. Miller, and J. F. Mitchell, Phys. Rev. B **71**, 014418 (2005).
[12] T. W. Beale *et al.*, Phys. Rev. B **72**, 064432 (2005).
[13] L. Brey and P. B. Littlewood, Phys. Rev. Lett. **95**, 117205 (2005); L. Brey, Phys. Rev. Lett. **92**, 127202 (2004).
[14] G. C. Milward *et al.*, Nature (London) **433**, 607 (2005).
[15] X. Z. Yu *et al.*, Phys. Rev. B **75**, 174441 (2007).
[16] A. Nucara *et al.*, Phys. Rev. Lett. **101**, 066407 (2008).
[17] D. Koumoulis *et al.*, Phys. Rev. Lett. **104**, 077204 (2010).
[18] S. Larochelle *et al.*, Phys. Rev. Lett. **87**, 095502 (2001).
[19] S. Larochelle *et al.*, Phys. Rev. B **71**, 024435 (2005).
[20] M. Pissas and G. Kallias, Phys. Rev. B **68**, 134414 (2003).
[21] P. Reutler *et al.*, J. Cryst. Growth **249**, 222 (2003).
[22] D. Senff *et al.*, Phys. Rev. Lett. **96**, 257201 (2006).
[23] D. Senff *et al.*, Phys. Rev. B **77**, 184413 (2008).
[24] B. J. Sternlieb *et al.*, Phys. Rev. Lett. **76**, 2169 (1996).
[25] The magnetic intensities in Fig. 4(b) are obtained by superposing the four domain contributions with a slight imbalance assuming magnetic moments forming an angle of 31° with the propagation of the zigzag chain and a reduced moment of the excess Mn^{4+}.
[26] A. T. Savici *et al.*, Phys. Rev. B **75**, 184443 (2007).